Thymoquinone protects against hyperlipemia-induced cardiac damage in low-density lipoprotein receptor-deficient (LDL-R−/−) mice

Zuowei Pei
Beijing Hospital
Ying Guo
Beijing Hospital
Huolan Zhu
Beijing Hospital;Peking Union Medical College
Min Dong
Bejing Hospital
Qian Zhang
Beijing Hospital
Fang Wang (bjh_wangfang@163.com)
Beijing Hospital

Research

Keywords: hyperlipemia, thymoquinone, cardiac damage, cardiovascular disease, low-density lipoprotein receptor deficient (LDL-R/) mice

Posted Date: April 28th, 2020

DOI: https://doi.org/10.21203/rs.3.rs-24669/v1

Abstract

Background Hyperlipemia is a risk factor for cardiac damage and cardiovascular disease. Several studies have shown that thymoquinone (TQ) can protect against cardiac damage. The aim of this study was to investigate the possible protective effects of TQ against hyperlipemia-induced cardiac damage in low-density lipoprotein receptor deficient (LDL-R−/−) mice.

Methods: Eight-week-old male LDL-R−/−mice were randomly divided into the following three groups: the control group fed a normal diet (ND group), the high fat diet (HFD) group, and the HFD mixed with TQ (HFD+TQ) group. All groups were fed the different diets for 8 weeks. Blood samples were obtained from the inferior vena cava, collected in serum tubes, and stored at -80 °C until use. Cardiac tissues were fixed in 10% formalin and then embedded in paraffin for histological evaluation. The remainder of the cardiac tissues was snap-frozen in liquid nitrogen for mRNA preparation or immunoblotting.

Results The levels of metabolism-related factors, such as total cholesterol (TC), low-density lipoprotein-cholesterol (LDL-c), and high-sensitivity C-reactive protein (hs-CRP), were decreased in the HFD+TQ group compared with that in the HFD group. Periodic acid-Schiff staining demonstrated that lipid deposition was lower in the HFD+TQ group than that in the HFD group. The expression of pyroptosis indicators (NOD-like receptor 3 [NLRP3], interleukin [IL]-1β, IL-18 and caspase-1), pro-inflammation factors (IL-6 and tumour necrosis factor alpha [TNF-α]), and macrophage markers (cluster of differentiation [CD]68) was significantly downregulated in the HFD+TQ group compared with that in the HFD group.

Conclusions Our results indicate that TQ may serve as a potential therapeutic agent for hyperlipemia-induced cardiac damage.

Introduction

Hyperlipemia is a critical damage-inducing element in cardiovascular disease (CVD) [1]; individuals with hyperlipidaemia have a higher risk of CVD compared with those with normal cholesterol levels [2]. Furthermore, increasing evidence has shown that dyslipidaemia-related cardiac damage is associated with lipid accumulation, oxidative stress, and inflammation [3, 4].

Several researchers have investigated various drugs for treating hyperlipidaemia such as statins; however, as these are related to the development of resistance in cells and as these are associated with adverse effects, new methods for treating hyperlipidaemia are needed. Thymoquinone (TQ) is the major constituent of *Nigella sativa* [5], commonly known as black seed or black cumin, and is globally used in folk (herbal) medicine for treating and preventing a number of diseases and conditions [6]. Previous studies have reported that TQ suppresses chronic cardiac inflammation [7], and regulates the expression of factors, such as vascular endothelial growth factor and nuclear factor-erythroid-2-related factor 2 (Nrf2), thereby improving the antioxidant potential of the cardiac muscle. In addition, TQ alleviates diabetes-associated oxidative stress in cardiac tissues [8]. Additionally, several studies have shown that the protective effect of TQ against cardiac damage such as in case of ischemic damage [9] and acute

abdominal aortic ischemia-reperfusion injury [10]is mediated via the pyroptosis pathway [11]. Recently, pyroptosis, an inflammatory form of programmed cell death [12], has been gaining increasing attention, especially during hyperlipemia [13, 14]; however, the pathophysiological mechanisms underlying the relationship between hyperlipemia and cardiac damage are not yet fully understood.

Therefore, in this study, we investigated the role of TQ in hyperlipidaemia-induced cardiac damage in a low-density lipoprotein receptor-deficient (LDL-R−/−) mouse model.

Methods

Animal model

LDL-R$^{-/-}$ mice were purchased from Beijing Vital River Lab Animal Technology CO., LTD. (Beijing, China). All mice were bred in a room with a 12/12-h light-dark cycle at a controlled temperature (24 – 26 °C). Male LDL-R−/− mice (8-week-old) were randomly divided into the following three groups: mice fed a normal diet (ND group, n = 8), mice fed a high-fat diet (HFD group, n = 8), and mice fed a high-cholesterol diet + 50 mg/kg/day of TQ (HFD+TQ group, n = 8). The experimental diet was purchased from Shanghai Slac Laboratory Animal Co., Ltd. (Shanghai, China). Mice in all groups were fed with the appropriate diet for 8 weeks. Blood samples were acquired from the inferior vena cava, collected in serum tubes, and stored at -80 °C until use. Cardiac tissues were fixed in 10% formalin and embedded in paraffin for histological evaluation. The remaining cardiac tissues were snap-frozen in liquid nitrogen for mRNA isolation and immunoblotting analyses. The animal experiment was approved by the Animal Ethics Committee of Beijing Hospital.

Biochemical measurements

Sera were separated from the collected blood samples by centrifugation at 3000 rpm for 15 min. The levels of total cholesterol (TC), low-density lipoprotein cholesterol (LDL-c) and high-sensitivity C-reactive protein (hs-CRP) in the serum were detected using the Total Cholesterol, low-density lipoprotein cholesterol, and high-sensitivity C-reactive protein Assay Kit (Nanjing Jiancheng Bioengineering Institute, Nanjing, China), as per the manufacturer's instructions.

Haematoxylin and eosin staining

The cardiac tissues were fixed with 10% buffered formalin for 30 min and then dehydrated in 75% ethanol overnight, followed by paraffin embedding. Serial sections (4 μm) were stained with haematoxylin and eosin for pathological analysis.

Periodic acid-Schiff (PAS) staining

Cardiac tissues from each group were stored in 10% formalin, dehydrated in an ascending alcohol series (75, 85, 90 and 100% alcohol, 5 min each) and then embedded in paraffin wax. Paraffin sections (4-μm-thick), sliced from these paraffin-embedded tissue blocks, were then de-paraffinized via immersion in

xylene (three times, 5 min each) and rehydrated using a descending alcohol series (100, 90, 85 and 75% alcohol, 5 min each). Samples were stained with PAS stain to investigate the changes in cardiac morphology. Red staining indicated lipid deposition.

Immunohistochemistry

Immunohistochemistry was performed according to the manufacturer's instructions (Zsbio, Beijing, China) with antibodies against cluster of differentiation (CD)68 (rabbit anti-CD68 antibody, 1:200; Proteintech, Wuhan, China) and CD36 (rabbit anti-CD36 antibody, 1:200; Proteintech). The results were visualised using an Olympus microscope (Olympus, Tokyo, Japan). NIH ImageJ software was used for quantification.

Western blotting

Protein samples obtained from cardiac tissues were electrophoresed on 10% sodium dodecyl sulphate-polyacrylamide gel electrophoresis (SDS-PAGE) gels and then transferred to polyvinylidene fluoride membranes (Immobilon, Millipore, Billerica, MA, USA). The membranes were blocked in Tris-buffered saline with 0.1% Tween-20 (TBS-T) containing 5% skimmed milk, and then incubated overnight with gentle shaking at 4 ℃ in a diluent (P0023A; Beyotime) containing primary antibodies against NOD-like receptor 3 (NLRP3; rabbit anti-NLRP3 antibody, 1:1000; Boster, Wuhan, China), interleukin [IL]-18 (rabbit anti- IL-18 antibody, 1:1000; Proteintech), IL-1β (rabbit anti- IL-1β antibody, 1:1000; Arigo, Hamburg, Germany), caspase-1 (rabbit anti-caspase-1 antibody, 1:1000; Proteintech), phospho-extracellular signal-related kinase (P-ERK; Rabbit anti- PI3K, 1:1000; Proteintech), and anti-β-actin (1:1000; Proteintech). The membranes were then incubated with a secondary antibody (anti-rabbit Ig-G, 1:1000; Cell Signaling Technology) for 1 h. This analysis was carried out independently three times. Protein levels are expressed as protein/β-actin ratios to minimise the loading differences. The relative signal intensity was quantified using NIH ImageJ software.

RNA isolation and real-time PCR (qPCR)

Total RNA was isolated from cardiac tissues and complementary DNA (cDNA) was synthesised using the TransScript One-Step gDNA Removal and cDNA Synthesis SuperMix kit (Transgen, Beijing, China) according to the manufacturer’s protocol. Gene expression was quantitatively analysed by qPCR using the TransStart Top Green qPCR SuperMix kit (Transgen). β-Actin was amplified and quantitated in each reaction in order to normalise the relative amounts of the target genes. Primer sequences are listed in Table 1.

Table 1 Primer oligonucleotide sequences

Gene	Primers
TNF-α	F:5′-TCTCATGCACCACCATCAAGGACT-3′ R:5′-ACCACTCTCCCTTTGCAGAACTCA-3′
IL-6	F:5′-TACCAGTTGCCTTCTTGGGACTGA-3′ R:5′-TAAGCCTCCGACTTGTGAAGTGGT-3′
NLRP3	F:5′- CTGCGGACTGTCCCATCAAT-3′ R:5′- AGGTTGCAGAGCAGGTGCTT-3′
IL-1β	F: 5′-TGCCACCTTTTGACAGTGAT-3′ R: 5′-TGTGCTGCTGCGAGATTTGA-3′
IL-18	F: 5′-ATGGCTGCTGAACCAGTAGAAG-3′ R: 5′- CAGCCATACCTCTAGGCTGGC-3′
Caspase-1	F: 5′-AACCAGGAGAATGTTTCCAACCT-3′ R: 5′-AAACACCAGGCCAAGCTTCTT-3′
β-actin	F:5′-CGATGCCCTGAGGGTCTTT-3′ R:5′-TGGATGCCACAGGATTCCAT-3′

Abbreviations: TNF-α, tumor necrosis factor-α; IL-6, interleukin- 6; NLRP3, the nucleotide-binding and oligomerization domain-like receptor 3; IL-18, interleukin- 18; IL-1β, interleukin- 1β

Statistical analysis

All data are presented as the mean ± standard error of mean (SEM). Statistical analysis was performed using SPSS software version 23.0 (SPSS Inc., Chicago, IL, USA). Inter-group variation was measured using one-way analysis of variance (ANOVA) and subsequent Tukey's test. The minimal level for statistical significance was set at $P < 0.05$.

Results

Metabolic Characterisation

The metabolic characteristics of LDL-R□/□ mice after 8 weeks of different treatments are summarised in Table 2. The heart/body weight ratio did not change in the three groups. TC, LDL-c and hs-CRP levels were markedly increased in the HFD group, but significantly decreased in the HFD + TQ group.

Table 2
Metabolic data from the four groups after 8 weeks of dietary treatment. Abbreviations: TC, total cholesterol; LDL-C, low-density lipoprotein- cholesterol

	LDL-R□/□ ND	LDL-R□/□ HFD	LDL-R□/□ HFD + TQ
Heart/BW(mg/g)	4.175 ± 0.1966	3.814 ± 0.3045	4.483 ± 0.08
TC(mmol/L)	8.5 ± 1.207*	34.01 ± 2.318	14.08 ± 0.7108*
LDL-c(mmol/L)	3.938 ± 0.1281*	23.88 ± 1.651	6.783 ± 0.6817*
Hs-crp(ng/dl)	58.5 ± 4.252*	221.2 ± 13.43	111.7 ± 10.19*#
Abbreviations: BW, body weight; TC, total cholesterol; LDL-C, low-density lipoprotein- cholesterol. Data are means ± SEM; n = 5–6 per group. * $P < 0.05$ vs LDL-R□/□ HFD; # $P < 0.05$ vs LDL-R□/□ ND.			

TQ reduced HFD-induced cardiac damage

To evaluate inflammatory cell infiltration into the cardiac tissue, haematoxylin and eosin staining was performed (Fig. 1). HFD+TQ group mice showed markedly reduced inflammatory cell infiltration in their cardiac tissue compared with that in the HFD group mice, indicating that TQ reduced HFD-induced cardiac damage.

To evaluate lipid accumulation in cardiac tissue, we evaluated PAS staining and the expression of CD36 and CD68 (Fig. 2). Increased lipid retention was detected in the cardiac tissues of HFD group mice. Interestingly, HFD +TQ group mice showed markedly reduced lipid deposition in the cardiac tissue compared with that in HFD group mice.

TQ reduced HFD-induced expression of pro-inflammatory cytokines in mouse cardiac tissues

To examine the involvement of pro-inflammatory cytokines in the cardiac tissues of the three groups of mice, mRNA expression of IL-6 and tumour necrosis factor alpha (TNF-α) was measured using qPCR (Fig. 3). Although IL-6 and TNF-α mRNA were upregulated in the HFD group, this upregulation was attenuated in the HFD+TQ group.

TQ reduced HFD-induced pyroptosis in cardiac tissues

To evaluate pyroptosis in cardiac tissues, we examined the mRNA and protein expression of pyroptosis indicators NLRP3, caspase-1, IL-1β, and IL-18 (Fig. 4). NLRP3, caspase-1, IL-1β and IL-18 mRNA was significantly downregulated in the HFD+TQ group compared with that in the HFD group (Fig. 4a). *Western blotting* (Fig. 4b) *demonstrated that the levels of* NLRP3, caspase-1, IL-1β, and IL-18 *were* markedly reduced in the cardiac tissues of the HFD+TQ group compared with that in the HFD group (Fig. 4b-c). These results indicate that TQ reduced HFD-induced upregulation of NLRP3, caspase-1, IL-1β, and IL-18 expression.

TQ reduced HFD-induced increase in *P-ERK* levels in the cardiac tissues of mice

To investigate the effect of TQ on the regulation of the *ERK* signalling pathway, we analysed *P-ERK* levels in the respective treatment groups by western blotting (Fig. 5). *P-ERK* level was higher in the HFD group than that in the ND group, and the HFD+TQ group exhibited significantly low *P-ERK* levels than the HFD group.

Discussion

The present study demonstrates that TQ has a protective effect against hyperlipemia-induced progressive lipid deposition, pro-inflammatory cytokine expression, and pyroptosis.

Metabolic characteristic analysis indicated that the levels of TC and LDL-c were increased in the HFD group compared to that in the ND group mice. These results are in agreement with reports by Kolbus *et al*. [15]. Interestingly, the TC and LDL-c levels in the HFD + TQ group were significantly lower than those in the HFD group. Several clinical studies have indicated that hs-CRP can serve as a biomarker for the risk prediction of cardiovascular events [16, 17]. Our results show that the HFD + TQ group had markedly reduced serum hs-CRP levels compared with that in the HFD group, indicating that TQ influences cholesterol metabolism and hs-CRP levels.

Hyperlipidaemia promotes macrophage accumulation and lipid deposition in cardiac tissues [18]. Cellular lipid homeostasis involves the regulation of influx, synthesis, catabolism, and efflux of lipids. An imbalance in these processes can result in the conversion of macrophages into foam cells [19]. The CD68 marker identifies a population of macrophages; CD68 positive cells are often observed infiltrating cardiac tissues [18]. The results of our lipid deposition assays showed that CD36 expression and PAS staining were significantly increased in the LDL-R−/− HFD group mice compared with that in the ApoE−/− ND mice; however, this damage was significantly inhibited in the HFD + TQ group.

Pro-inflammatory cytokines have been reported to be highly expressed in hyperlipidaemia, and are known to contribute to cardiac damage [20, 21]. Our study showed that the expression of IL-6, and TNF-α was reduced in the HFD + TQ group compared with that in the HFD group, indicating that TQ downregulated HFD-induced expression of IL-6 and TNF-α.

Pyroptosis is a novel programmed cell death mechanism. Recent studies have reported that pyroptosis contributes to the development of hyperlipidaemia. Pyroptosis induction is closely associated with the activation of the NLRP3 inflammasome, which has been linked to key cardiovascular risk factors including hyperlipidaemia [22, 23]. A significant decrease in atherosclerotic lesion size has also observed at the aortic sinus of HFD-fed LDL-R−/− mice reconstituted with NLRP3 knockout bone marrow cells [23]. In addition, previous studies have shown that NLRP3 recruits caspase-1, leading to the activation of caspase-1, maturation and secretion of IL-1β and IL-18, and initiation of pyroptosis [24–27]. Our results showed that the cardiac tissues in the HFD + TQ group expressed markedly reduced levels of NLRP3, caspase-1, IL-1β and IL-18 compared with that in the HFD group, indicating that TQ downregulated HFD-induced pyroptosis.

ERK is a cytoplasmic kinase whose activity is regulated by phosphatases [28]. Previous studies have suggested that TQ increases the phosphorylation of mitogen-activated protein kinases and ERK [29]. P-ERK modulates cellular metabolism by a series of reactive oxygen stress activities. TQ increases P-ERK levels to regulate cellular activity [30]. Our study showed that P-ERK levels decreased in the HFD group, but were significantly increased in the HFD + TQ group.

Conclusions

Our data establish that TQ contributes to the mitigation of hyperlipidaemia-induced cardiac damage, as shown by reduced lipid deposition and pyroptosis and downregulated pro-inflammatory cytokine

expression. These findings provide new insights into the role of TQ in hyperlipidaemia-induced cardiac damage and introduce the possibility of a novel therapeutic intervention for treating CVDs.

Abbreviations

TQ: thymoquinone; LDL-R$^{-/-}$: low-density lipoprotein receptor deficient; ND: normal diet; HFD: high fat diet; TC: total cholesterol; LDL-c: low-density lipoprotein-cholesterol; hs-CRP: high-sensitivity C-reactive protein; NLRP3; NOD-like receptor protein 3; IL: *interleukin;* TNF-α: tumour necrosis factor alpha; CD: cluster of differentiation; CVD: cardiovascular disease; Nrf2: nuclear factor-erythroid-2-related factor 2; PAS: periodic acid-Schiff; SDS-PAGE: sodium dodecyl sulphate-polyacrylamide gel electrophoresis; TBS-T: Tris-buffered saline with 0.1% Tween-20; P-ERK: phospho-extracellular signal-related kinase; cDNA: complementary DNA; qPCR: real-time PCR; SEM: standard error of mean; ANOVA: analysis of variance

Declarations

Ethics approval and consent to participate

All animal experiments were approved by the Ethics Committee of Beijing Hospital.

Consent for publication

Not applicable

Availability of data and materials

All datas generated or analyzed during this study are included in this published article.

Competing interests

The authors declare that they have no competing interests.

Funding

This study was funded by the 13th Five-year National Science and Technology Major Project (NSTMP; 2017ZX09304026).Capital Health Development Research Project (CHDRP, BJ-2016-071).

Authors' contributions

Fang Wang conceived the idea; Zuowei Pei and Ying Guo performed the experiments; Fang Wang and Min Dong analyzed the data; Zuowei Pei wrote the manuscript. Qian Zhang revised the manuscript. All authors have read and approved the final manuscript.

Acknowledgements

Not applicable.

Authors' information

Department of Cardiology, Beijing Hospital, National Center of Gerontology, Institute of Geriatric Medicine, Chinese Academy of Medical Sciences, Beijing, 100730, China

Zuo-Wei Pei, Ying Guo, Huo-Lan Zhu, Min Dong, Qian Zhang, Fang Wang

Peking Union Medical College, Chinese Academy of Medical Science, Beijing, 100730, China

Huo-Lan Zhu

References

1. Han Q, Yeung SC, Ip MSM, Mak JCW. Dysregulation of cardiac lipid parameters in high-fat high-cholesterol diet-induced rat model. Lipids Health Dis. 2018;17(1):255.
2. Karr S. Epidemiology and management of hyperlipidemia. Am J Manag Care. 2017;23(9 Suppl):139–48.
3. Wang B, Zhang S, Wang X, Yang S, Jiang Q, Xu Y, Xia W. Transcriptome analysis of the effects of chitosan on the hyperlipidemia and oxidative stress in high-fat diet fed mice. Int J Biol Macromol. 2017;102:104–10.
4. Chernukha IM, Fedulova LV, Kotenkova EA, Takeda S, Sakata R. Hypolipidemic and anti-inflammatory effects of aorta and heart tissues of cattle and pigs in the atherosclerosis rat model. Anim Sci J. 2018;89(5):784–93.
5. Asgharzadeh F, Bargi R, Beheshti F, Hosseini M, Farzadnia M, Khazaei M. Thymoquinone Prevents Myocardial and Perivascular Fibrosis Induced by Chronic Lipopolysaccharide Exposure in Male Rats: - Thymoquinone and Cardiac Fibrosis. J Pharmacopuncture. 2018;21(4):284–93.
6. Ali BH, Blunden G. Pharmacological and toxicological properties of Nigella sativa. Phytother Res. 2003;17(4):299–305.
7. Ghazwani M, Zhang Y, Gao X, Fan J, Li J, Li S. Anti-fibrotic effect of thymoquinone on hepatic stellate cells. Phytomedicine. 2014;21(3):254–60.
8. Atta MS, El-Far AH, Farrag FA, Abdel-Daim MM, Al Jaouni SK, Mousa SA. Thymoquinone Attenuates Cardiomyopathy in Streptozotocin-Treated Diabetic Rats. *Oxid Med Cell Longev* 2018, 2018:7845681.
9. Pu Q, Gan C, Li R, Li Y, Tan S, Li X, Wei Y, Lan L, Deng X, Liang H, et al. Atg7 Deficiency Intensifies Inflammasome Activation and Pyroptosis in Pseudomonas Sepsis. J Immunol. 2017;198(8):3205–13.
10. Liu H, Sun Y, Zhang Y, Yang G, Guo L, Zhao Y, Pei Z. Role of Thymoquinone in Cardiac Damage Caused by Sepsis from BALB/c Mice. Inflammation. 2019;429(2):516–25.
11. Lindblad A, Persson K, Demirel I. IL-1RA is part of the inflammasome-regulated immune response in bladder epithelial cells and influences colonization of uropathogenic E. coli. Cytokine.

2019;123:154772.

12. She Y, Shao L, Zhang Y, Hao Y, Cai Y, Cheng Z, Deng C, Liu X. Neuroprotective effect of glycosides in Buyang Huanwu Decoction on pyroptosis following cerebral ischemia-reperfusion injury in rats. J Ethnopharmacol. 2019;242:112051.
13. Zhang Y, Li X, Pitzer AL, Chen Y, Wang L, Li PL. Coronary endothelial dysfunction induced by nucleotide oligomerization domain-like receptor protein with pyrin domain containing 3 inflammasome activation during hypercholesterolemia: beyond inflammation. Antioxid Redox Signal. 2015;22(13):1084–96.
14. Yin Y, Li X, Sha X, Xi H, Li YF, Shao Y, Mai J, Virtue A, Lopez-Pastrana J, Meng S, et al. Early hyperlipidemia promotes endothelial activation via a caspase-1-sirtuin 1 pathway. Arterioscler Thromb Vasc Biol. 2015;35(4):804–16.
15. Kolbus D, Ramos OH, Berg KE, Persson J, Wigren M, Bjorkbacka H, Fredrikson GN, Nilsson J. CD8 + T cell activation predominate early immune responses to hypercholesterolemia in Apoe$^{-/-}$ mice. BMC Immunol. 2010;11:58.
16. Matsushita K, Yatsuya H, Tamakoshi K, Yang PO, Otsuka R, Wada K, Mitsuhashi H, Hotta Y, Kondo T, Murohara T, Toyoshima H. High-sensitivity C-reactive protein is quite low in Japanese men at high coronary risk. Circ J. 2007;71(6):820–5.
17. Shimada K, Fujita M, Tanaka A, Yoshida K, Jisso S, Tanaka H, Yoshikawa J, Kohro T, Hayashi D, Okada Y, et al. Elevated serum C-reactive protein levels predict cardiovascular events in the Japanese coronary artery disease (JCAD) study. Circ J. 2009;73(1):78–85.
18. Zhang X, Liu H, Hao Y, Xu L, Zhang T, Liu Y, Guo L, Zhu L, Pei Z. Coenzyme Q10 protects against hyperlipidemia-induced cardiac damage in apolipoprotein E-deficient mice. Lipids Health Dis. 2018;17(1):279.
19. Glass CK, Witztum JL. Atherosclerosis. the road ahead. Cell. 2001;104:503–16.
20. Baker RG, Hayden MS, Ghosh S. NF-kappaB, inflammation, and metabolic disease. Cell Metab. 2011;13(1):11–22.
21. Mathias D, Mitchel RE, Barclay M, Wyatt H, Bugden M, Priest ND, Whitman SC, Scholz M, Hildebrandt G, Kamprad M, Glasow A. Correction: Low-Dose Irradiation Affects Expression of Inflammatory Markers in the Heart of ApoE $^{-/-}$ Mice. PLoS One. 2016;11(6):e0157616.
22. Abela GS, Aziz K. Cholesterol crystals rupture biological membranes and human plaques during acute cardiovascular events–a novel insight into plaque rupture by scanning electron microscopy. Scanning. 2006;28(1):1–10.
23. Duewell P, Kono H, Rayner KJ, Sirois CM, Vladimer G, Bauernfeind FG, Abela GS, Franchi L, Nunez G, Schnurr M, et al. NLRP3 inflammasomes are required for atherogenesis and activated by cholesterol crystals. Nature. 2010;464(7293):1357–61.
24. Goncalves AC, Ferreira LS, Manente FA, de Faria C, Polesi MC, de Andrade CR, Zamboni DS, Carlos IZ. The NLRP3 inflammasome contributes to host protection during Sporothrix schenckii infection. Immunology. 2017;151(2):154–66.

25. Bordon Y. Mucosal immunology: Inflammasomes induce sepsis following community breakdown. Nat Rev Immunol. 2012;12(6):400–1.
26. Liston A, Masters SL. Homeostasis-altering molecular processes as mechanisms of inflammasome activation. Nat Rev Immunol. 2017;17(3):208–14.
27. Borges PV, Moret KH, Raghavendra NM, Maramaldo Costa TE, Monteiro AP, Carneiro AB, Pacheco P, Temerozo JR, Bou-Habib DC, das Gracas Henriques M, Penido C. Protective effect of gedunin on TLR-mediated inflammation by modulation of inflammasome activation and cytokine production: Evidence of a multitarget compound. *Pharmacol Res* 2017, 115:65–77.
28. Wainstein E, Seger R. The dynamic subcellular localization of ERK: mechanisms of translocation and role in various organelles. Curr Opin Cell Biol. 2016;39:15–20.
29. El-Najjar N, Chatila M, Moukadem H, Vuorela H, Ocker M, Gandesiri M, Schneider-Stock R, Gali-Muhtasib H. Reactive oxygen species mediate thymoquinone-induced apoptosis and activate ERK and JNK signaling. Apoptosis. 2010;15(2):183–95.
30. Bouhlel A, Ben Mosbah I, Hadj Abdallah N, Ribault C, Viel R, Mannai S, Corlu A, Ben Abdennebi H. Thymoquinone prevents endoplasmic reticulum stress and mitochondria-induced apoptosis in a rat model of partial hepatic warm ischemia reperfusion. Biomed Pharmacother. 2017;94:964–73.

Figures

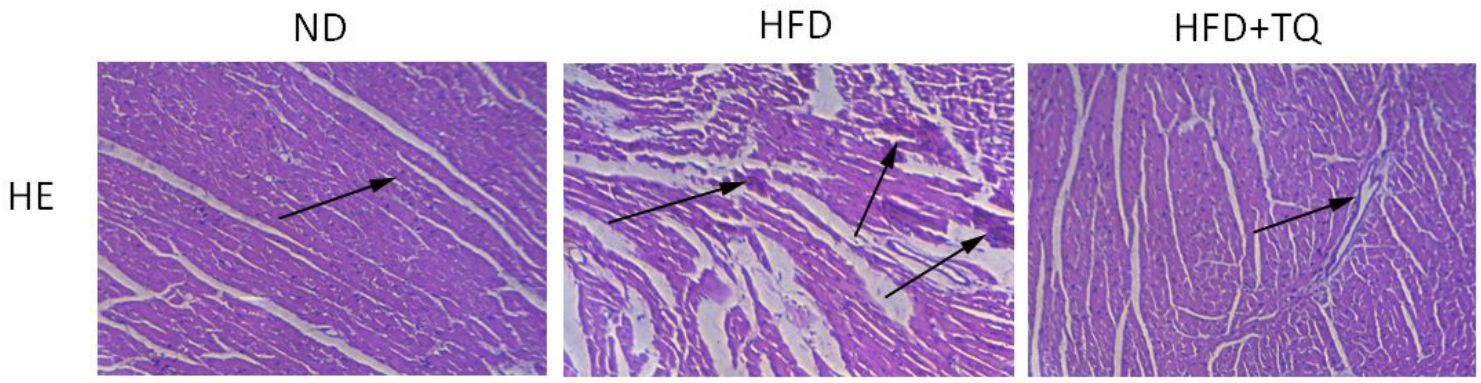

Figure 1

Effect of TQ on hyperlipidaemia-induced histopathological changes in the cardiac tissues. HE staining in cardiac tissues of three group with different treatments. Magnification 40 X. The arrows indicate damage. n=3 per group

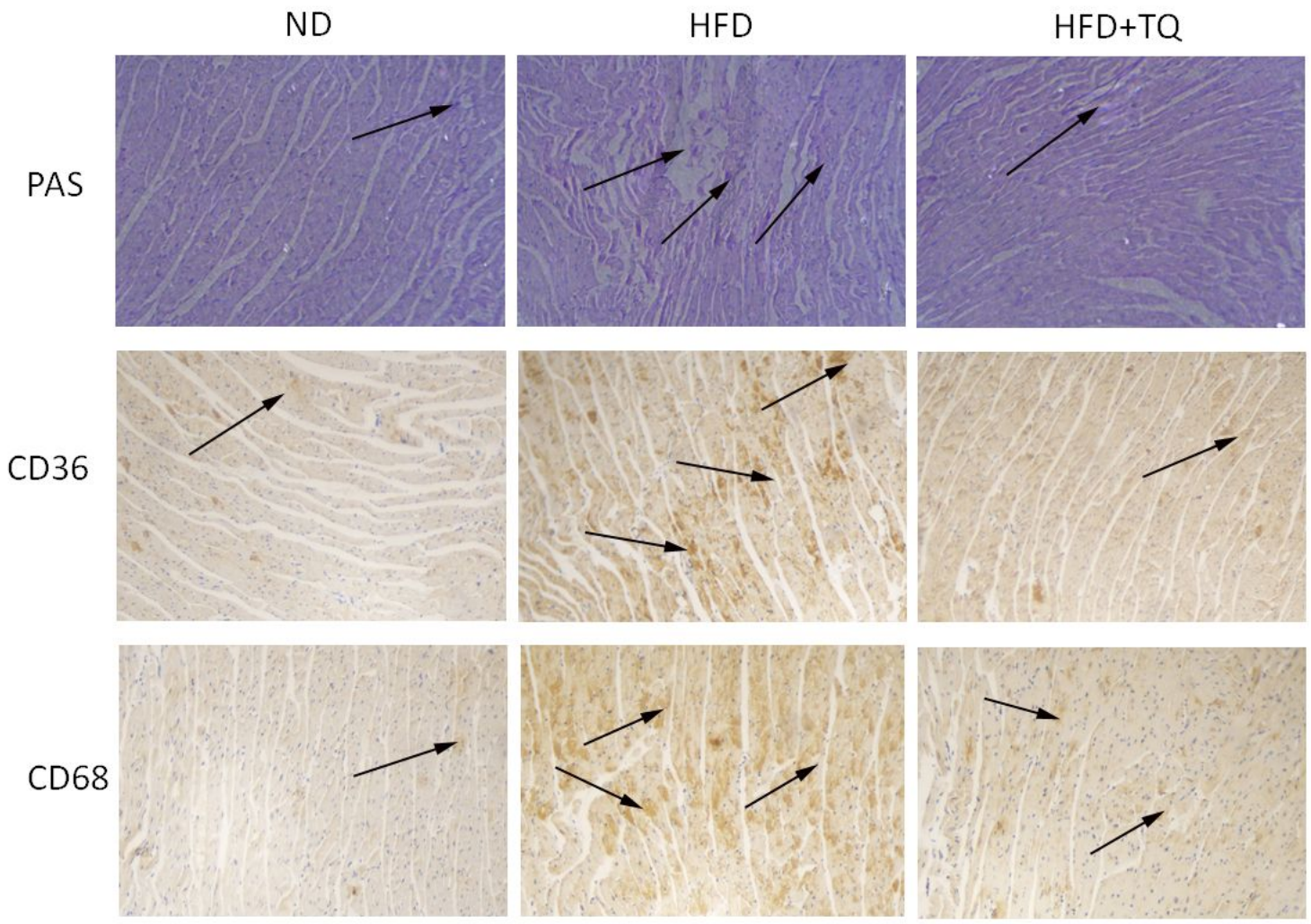

Figure 2

Effect of TQ on hyperlipidaemia-induced lipid accumulation in the cardiac tissues. PAS, CD36 and CD68 staining in cardiac tissues of three group with different treatments. Magnification 40 X. The arrows indicate damage. n=3 per group

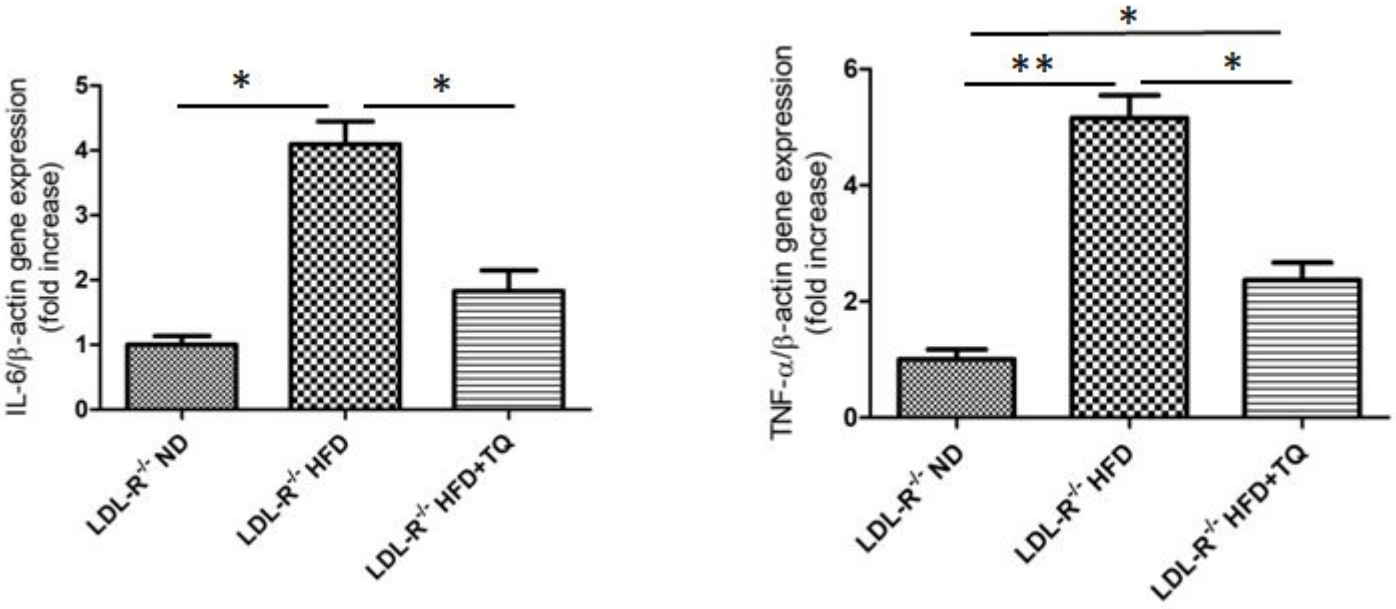

Figure 3

Pro-inflammatory gene expression in the cardiac tissue. Relative mRNA expression of TNF-α and IL-6 in cardiac tissue of three group with different treatments. Data are given as the means ± SEM; n = 5-6 in each group. * P < 0.05 ; **P < 0.01

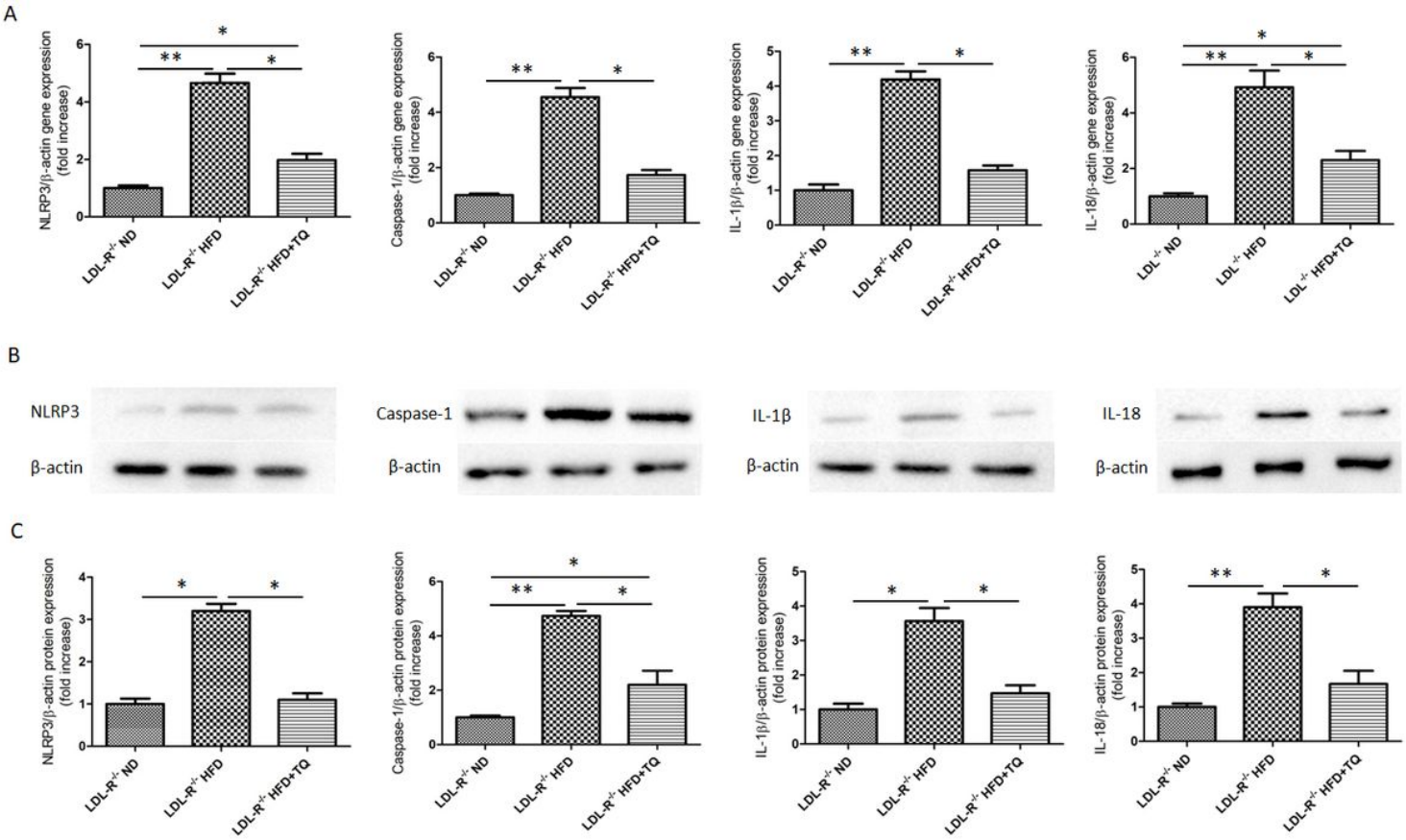

Figure 4

Pyroptosis expression in the cardiac tissues. (A) Relative mRNA expression of NLRP3, caspase-1, IL-1β, and IL-18 in cardiac tissue of three group with different treatments. (B) Immunoblotting for NLRP3, caspase-1, IL-1β, and IL-18 protein expression in cardiac tissues. (C) Bar graph showing quantification of NLRP3, caspase-1, IL-1β, and IL-18 protein expression. Data are given as the means ± SEM; n = 5-6 in each group. * P < 0.05, **P < 0.01

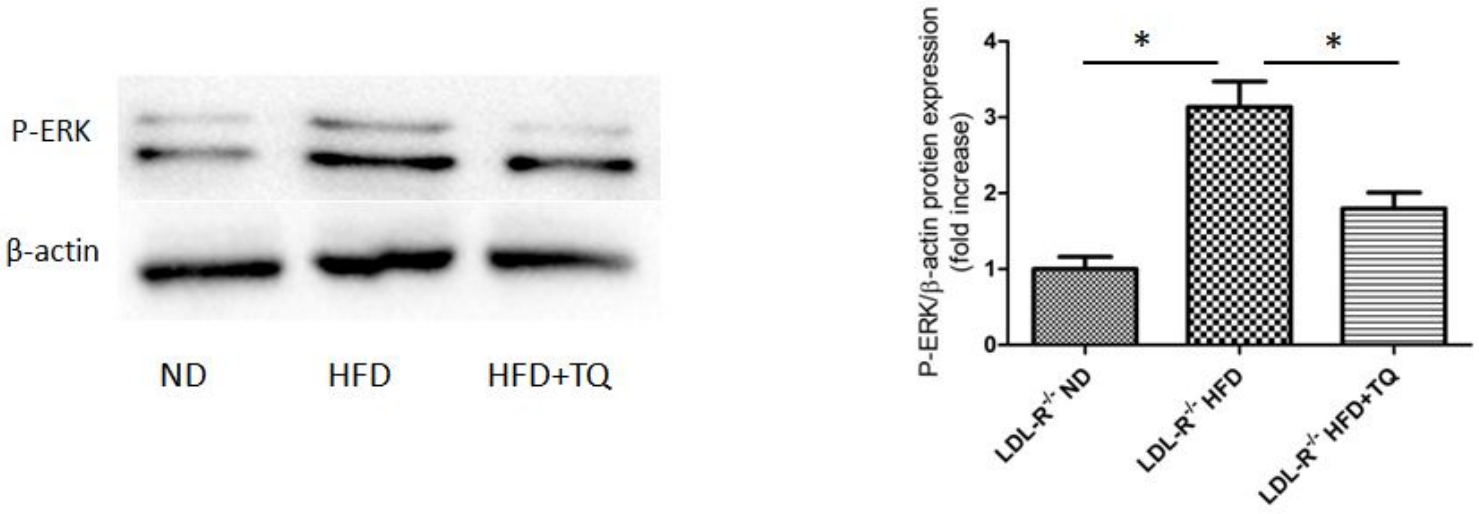

Figure 5

Phospho-ERK expression in the cardiac tissues. (A) Immunoblotting for phospho-ERK levels in cardiac tissues. (B) Bar graph shows the quantification of phospho-ERK levels. Data are given as the means ± SEM; n = 3 in each group. *P < 0.05